Available online at www.sciencedirect.com

ScienceDirect

Advances in Space Research 58 (2016) 92–107

ADVANCES IN SPACE RESEARCH
(a COSPAR publication)

www.elsevier.com/locate/asr

Nighttime thermospheric meridional winds as inferred from ionosonde parameters over Indian region and their plausible effects on plasma irregularities

Sreeba Sreekumar, S. Sripathi *

Indian Institute of Geomagnetism, Navi Mumbai, India

Received 1 January 2016; received in revised form 6 April 2016; accepted 7 April 2016
Available online 16 April 2016

Abstract

In this paper, we present nighttime thermospheric meridional winds at Indian low latitude station namely Hyderabad during March–May 2013 derived using (a) h'F method and (b) hpF2 method based on ionosondes. The estimation of meridional winds using h'F method employs the basic principle that the vertical drift at magnetic equator is purely due to ExB drift, while for a station slightly away from magnetic equator, meridional wind also contributes for the vertical drift in addition to diffusion along the field lines. Assuming the EXB drifts are the same at both the locations, the vertical drift contribution is subtracted from the equatorial vertical drifts and then meridional winds are derived, whereas in hpF2 method, winds are derived using the SERVO theory. The winds so derived are compared with HWM07 wind model. The comparison suggests that magnitude of winds derived using h'F method are in better agreement with HWM07 model than hpF2 derived winds where their polarities are better comparable to HWM07 model than hpF2 method. The poor agreement of hpF2 method could be due to uncertainties involved in estimating various ionospheric parameters. Also the winds derived using h'F method showed signatures of the well known phenomenon of Midnight Temperature Maximum (MTM). Based on these results, we suggest that h'F method is better suited for meridional wind estimates over low latitudes than hpF2 method. Accordingly, we further investigated the role of thermospheric meridional winds in equatorial spread F (ESF) occurrence. Our results suggest that equatorward winds along with post sunset height increase could enhance the Rayleigh Taylor (RT) instability growth rate and thereby leading to the generation of ESF/scintillations. The Superposed Epoch Analysis (SEA) technique has been applied to understand the general trend of h'F and meridional winds around the ESF onset time. The study showed reduction in poleward winds, half an hour prior to the onset of ESF. Hence indicating the role of meridional winds in the generation of plasma irregularities/scintillations in addition to post sunset height rise.

Keywords: Night time thermospheric meridional winds; ESF irregularities

1. Introduction

The equatorial Thermosphere–Ionosphere act as a coupled system, whereby an interactive coupling between plasma and neutrals exists. As a result, it helps in transporting energy and momentum throughout the system. It is well known that neutral winds and electric fields controls the distribution of plasma density in the E and F regions. The thermospheric neutral winds, i.e., zonal wind, through the dynamo process results in the generation of electric fields during the post sunset hours leading to various phenomena in the evening equatorial and low latitude ionosphere; meridional component of neutral wind, being parallel to the magnetic field lines will cause changes in the F layer heights. It is well known that during post sunset

* Corresponding author.
E-mail address: ssripathi.iig@gmail.com (S. Sripathi).

http://dx.doi.org/10.1016/j.asr.2016.04.009
0273-1177/

period, considerable variations in the upward plasma drifts and thermospheric neutral winds occurs as a day to day, seasonal, solar flux and magnetic activity related variabilities (Fejer, 1991). Hence the meridional neutral winds plays a significant role in causing the variabilities associated with the different processes in the ionosphere and their study can lead to the understanding of various coupling processes between thermosphere and ionosphere system.

The importance of ESF studies and their variabilities have been closely associated with the global communication and navigation systems. Scintillations are the direct result of plasma density depletions which can cause tremendous impact on radio signals passing through the ionosphere. Subsequently, the prediction of ESF/scintillation occurence is of great significance and it can be easier, if the causative factors of its day to day variabilities are thoroughly understood. This marks the importance of knowledge of meridional winds and their variations in the F region heights since they are one of the major contributors to the day to day variabilities of ESF.

Several researchers have reported the estimation of meridional winds using different techniques. Ground based optical techniques were used, in which the direct measurements of airglow emissions at ionospheric heights (Meriwether et al., 1973; Sipler et al., 1983; Sahai et al., 1992) were obtained. Although they can provide both zonal as well as meridional wind components to a good accuracy, their availability is limited to some stations. Further, the observation using Fabry Perot Interferometer (FPI) is limited to nighttime measurements. One of the old, indirect technique is the meridional wind estimation from ion velocity measurements using Incoherent Scatter Radars (ISR) (Salah and Holt, 1974; Biondi et al., 1988; Harper, 1973; Burnside et al., 1983). However, the difficulty in wind measurements using this technique is again the fewer number of ISR's worldwide. Another indirect method is the estimation of meridional winds using ionospheric F-region height parameters scaled from ionograms recorded by ground-based ionosondes (Bittencourt and Sahai, 1978; Titheridge, 1995; Buonsanto et al., 1997; Liu et al., 2003). In Indian sector, using h'F data (Murthy et al., 1990) reported a method deriving night time thermospheric meridional winds. Using rocket experiments of Barium and Strontium cloud releases at SHAR, the method was further validated by Sekar and Sridharan (1992). One of the important method, SERVO Method which serves the purpose of description of the F2 peak behaviour has been developed by Rishbeth (1967). Since the meridional winds affect the movement of F2 peak, a further modification of this method by Rishbeth et al. (1978) and Ganguly et al. (1980) has been widely used by various researchers. For the low latitudes, some reports regarding the estimation of winds and variation in F2 peak has been obtained by Sridharan et al. (1991) and Gurubaran and Sridharan (1993) etc. While at mid latitudes, Miller et al. (1986), Medeiros et al. (1997) and Muella et al. (2008) have shown the wind variations using the parameters like hmF2, hpF2 etc. Nevertheless, some uncertainities can exist in ionosonde estimation of winds, the method is simpler than direct measurements and there are quite large number of ionosonde networks available throughout the world.

Meridional winds thus estimated using variety of instruments can be used in understanding the implications of variability of the well known phenomenon, namely Equatorial Spread F (ESF). As we know, the evening equatorial–low latitude ionosphere is unstable to density perturbations. This along with Rayleigh Taylor (RT) instability develops density irregularities which covers the scale sizes from centimetres to hundreds of kilometres leading to the phenomenon of Equatorial Spread F (ESF). ESF shows variability in season, local time, geographical location, solar activity etc as reported by various authors (Sastri et al., 1979; Fejer and Kelley, 1980; Rastogi, 1980; Abdu et al., 1981; Aarons, 1993; Sultan, 1996; Basu and Coppi, 1999; Huang et al., 2002). However, it exhibits day to day variability as well. Though enough advances has made in understanding the day to day variability of ESF, still it remains as a continuing puzzle. Some of the drivers of these variabilities include PRE electric field, meridional/transequatorial neutral winds and gravity waves acting as seed perturbations.

Hence, out of the many factors controlling the onset, development and variabilities of ESF, meridional/transequatorial winds are those which have significant role to be played in either assisting/suppressing them in a day to day basis. So, the estimation and further observations of these winds over F region heights can resolve the problem of day to day variability of ESF, Equatorial Ionization Anomaly (EIA) etc. Recent study by Huba and Krall (2013), using NRL 3D equatorial spread F code SAMI3/ESF shows that it is not necessary that meridional winds cause a stabilizing effect on ESF onset, rather they can have destabilizing response. They mentioned the effect as a function of latitude, ie., a positive gradient wind profile as a function of latitude results in a stabilizing influence on the generalized RT instability; while that with a negative gradient leads to a destabilizing effect. The polarity of the wind is an important parameter controlling the height of F layer especially in the low-mid latitudes, where the electric field impact is considered to be less significant, unlike equatorial latitudes. Poleward wind would inhibit ESF by pushing the F-region ionization to lower altitudes along the magnetic field lines, which would enhance the E-region conductivities and, hence, loading the F-region dynamo field and inhibiting the uplift of the F-layer (Maruyama, 1988; Mendillo et al., 1992). Using the NRL SAMI3 code, (Krall et al., 2009) showed that for a sufficiently large constant meridional wind of the order of 60 m/s, RT instability and hence ESF can be stabilized. The importance of polarity of wind in terms of the critical height of the F layer has been reported by Devasia et al. (2002) during a study on March–April period of 1998 which suggests that when h'F is less than a critical height of 300 km, equatorward wind is necessary for bottomside spread F generation. Likewise the meridional wind control on ESF onset, scintillations are also affected by the polarity/magnitude of meridional winds.

Present study deals with the estimations of the night time thermospheric meridional winds during the equinoctial months (March–April) of the year 2013. The winds were estimated using ionosonde height parameters, like h'F and hpF2, obtained from observations in the equatorial station of Tirunelveli (TIR) and in the low latitude station of Hyderabad (HYD), both in the Indian region. The uniqueness in our study is that Superposed Epoch Analysis (SEA) technique has been applied to understand the general behaviour of winds. SEA, regarding its application to obtain the effect of meridional winds on ESF control/generation has been rarely reported earlier. So far, MLT region winds (Singer et al., 1994) and geomagnetic storm studies (Yokoyama and Kamide, 1997; Hutchinson et al., 2011) are the areas mainly dealt with this method. Although, h'F vs meridional wind analysis for ESF has been obtained in previous studies, we further extend the study by including the ESF/scintillation durations, which will give further insight into their association with meridional winds. In brief, the present study focuses on the meridional wind estimation, its comparison with another method and HWM07 model as well as an attempt to understand its role in causing variabilities to ESF.

2. Data and methods of analysis

2.1. h'F method for obtaining meridional winds

In this method, we have derived the night time thermospheric meridional winds over Hyderabad using h'F values obtained from two ionosondes. One is located in the equatorial region Tirunelveli (8.73°N, 77.7°E, Dip Lat = 0.3°S) and other station, Hyderabad (17.38°N, 78.45°E, Dip Lat = 12°N) is slightly away from the equator. Hereafter, the equatorial station, Tirunelveli is denoted as TIR, whereas the low latitude station, Hyderabad is denoted as HYD. Fig. 1 shows the geographical map of the locations of ionosonde stations. Here we adopt the method developed by Murthy et al. (1990). Principle behind the method is that at night time, the vertical drift at the equator will be only due to electrodynamic drift (E*X*B drift), but for stations slightly away from equator the vertical drift will be affected by diffusion along the field lines as well as due to meridional winds. Thus meridional winds are having significant influence over low latitude stations and their influence depends on the dip angle (inclination angle), 'I' of the region.ie., low latitude station should have higher dip latitude value which comes in the range of 8–15° will be sufficient for meridional wind influence to be noted (Murthy et al., 1990). Hence Hyderabad station is suitable for estimating winds using this method. A geographical map of the ionosonde locations used in the investigation is shown in Fig. 1.

Coming to data analysis part, we have considered approximately 18 and 20 days from March and April, respectively to serve the purpose of simultaneity of data from both stations. The h'F values from the ionograms over TIR and HYD has been scaled for 4 and 4.5 MHz frequencies. This has been done so as to reduce the error in further calculations. While former station data had a time resolution of 10 min, latter had 20 min time resolution. In order to understand the geomagnetic disturbances, for the magnetic Ap index >15 was considered here as disturbed days. Some case studies for the three months of March, April and May are undertaken. March and April h'F values are of twenty minutes and ten minutes time resolution, respectively. The meridional wind directions by convention in the northern hemisphere are considered to be positive for poleward (northward) direction and negative for equatorward (southward).

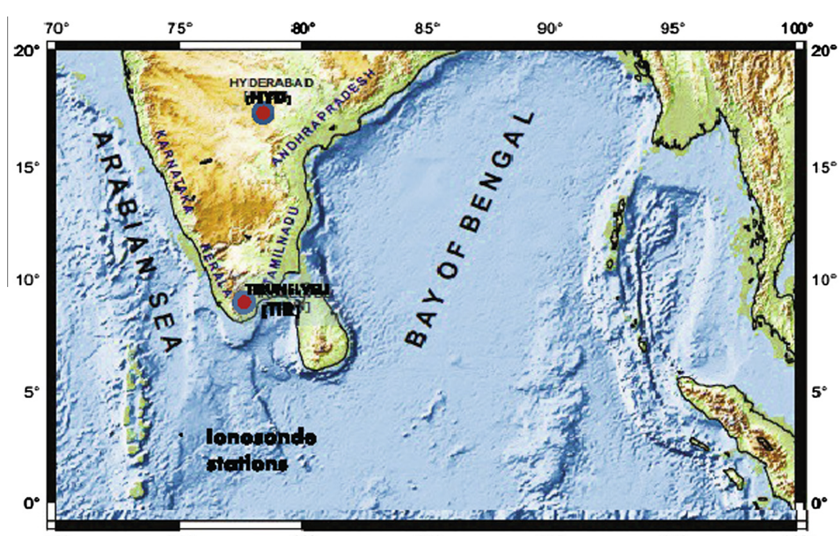

Fig. 1. Geographical map of the ionosonde stations used in the study.

The basic equations governing the estimation of winds are: Vertical drift velocity, given as the time rate of change of virtual height of F layer

$$V_o = \frac{d(h'F)}{dt} \tag{1}$$

The vertical drift, $\frac{d(h'F)}{dt}$ has been obtained for two frequencies 4 and 4.5 MHz for each stations. The electrodynamic drift at Tirunelveli (TIR) and Hyderabad (HYD) are denoted as V_T and V_H

$$V_T = V_{oT} - \beta_{oT} H_{oT} \tag{2}$$

$$V_H = V_{oH} - \beta_{oH} H_{oH} \tag{3}$$

where V_{oT} and V_{oH} denotes the vertical drift at TIR and HYD and β_{oT} and β_{oH} are the effective chemical loss coefficients (attachment coefficient) at TIR and HYD. When h'F is at lower altitudes, the term β_{oT} and β_{oH} represent the apparent effects in the vertical drift velocity due to chemical loss. Hence, as mentioned by Bittencourt and Abdu (1981), 300 km is used as threshold height to calculate such apparent velocities in V_T and V_H. The terms β_{oT} and β_{oH} are obtained from the following equation

$$\beta = K_1(N_2) + K_2(O_2) \tag{4}$$

where β represents the effective chemical loss coefficients. K_1 and K_2 are the temperature dependent reaction rates involving N_2 and O_2. (N_2) and (O_2) are the number densities of N_2 and O_2, respectively, which are obtained from MSIS-E-90 model. Both K_1 and K_2 are obtained from Anderson and Rusch (1980) and given as:

$$K_1 = 2 * 10^{-11} * \left(\frac{T_n}{300}\right)^{-1/2} \tag{5}$$

$$K_2 = 1 * 10^{-10} \tag{6}$$

and both of which are expressed in cm^3/s. T_n is the neutral temperature as obtained from MSIS-E-90 model.

The Ionization Scale height, H is given as,

$$H = \left(\frac{1}{N} * \frac{dN}{dH}\right)^{-1} \tag{7}$$

where N is the background electron density. In order to obtain H_{oT} and H_{oH}, the heights of reflection at 4 and 4.5 MHz has been considered for both stations.

The horizontal component of the thermospheric neutral wind aligned with the geomagnetic field is given as U_m. i.e.,

$$U_m = 2\left(\frac{V_T \cos I - V_H}{\sin 2I}\right) - W_D \tan I \tag{8}$$

W_D is the plasma diffusion drift term as given by Rishbeth et al. (1978) and can be obtained from the vertical plasma velocity at F2 peak as,

$$V_{zm} = W - \left(\frac{g}{v_m}\right)\sin^2 I = W - \left(\frac{D_m}{2H}\right)\sin^2 I \tag{9}$$

Here, W is the vertical plasma drift applied to the layer by wind/electric field. g is the accelaration due to gravity. v denotes the ion-neutral collision frequency. D is the plasma diffusion coefficient given by

$$Dv = 2gH \tag{10}$$

Hence, on rearrangement,

$$W_D \tan I = \frac{g}{v_{in}} \tan(I) \tag{11}$$

g and v_{in} denotes the acceleration due to gravity and ion neutral collision frequency respectively. Here v_{in} is obtained from Banks and Kockarts (1973) and is given as,

$$v_{in} = 2.6 \times 10^{-9} \times (N_2) \times sqrt\left(\frac{\alpha_{O\_N_2}}{\mu_1}\right) + (O_2) \times sqrt\left(\frac{\alpha_{O\_O_2}}{\mu_2}\right) + (O) \times sqrt\left(\frac{\alpha_{O\_O}}{\mu_3}\right) \tag{12}$$

$\alpha_O\_N_2, \alpha_O\_O_2$ and α_O_O denotes the polarizability of O_N_2, O_O_2 and O_O respectively. μ_1, μ_2 and μ_3 represents the reduced masses of O+ and N_2, O+ and O_2 and O+ and O.

2.2. hpF2 method-an adaptation of servo model

This method provides a description of conditions at the F2 peak by providing the effect of meridional neutral winds on them. It is mentioned earlier that the polarity of winds has a significant part to play in causing the F peak variations. This method is mainly based on the SERVO method developed by Rishbeth et al. (1978). The main principle involved in the method is as described: The night time F2 peak will be at a stationary level 'h_s', where the loss rate due to recombination of plasma equals the rate of plasma diffusion. This is the case in the absence of any external forcing on the ionization vertical drift and the stationary height is given by,

$$\beta_s = \frac{kD_s \sin^2(I)}{2H^2(kac - 1)} \tag{13}$$

k is the ratio of molecular to atomic masses, i.e., the loss scale height factor, I refers to the dip angle (inclination angle) of the low latitude station. a is the layer shape factor and c is the empirical constant that helps in adjusting the loss and transport of plasma at F2 peak height. D_s is the ambipolar plasma diffusion coefficient that apply to the height h_s. Atomic Oxygen scale height at F2 peak is given by,

$$H = 0.058T_n \tag{14}$$

T_n denotes the neutral temperature.

Chemical loss coefficient that apply to the stationary height h_s is given by,

$$\beta_s = K_1(N_2) + K_2(O_2) \tag{15}$$

$$D_s = R(T_i + T_e)/(16K_1[O] + 28K_2[N2]) \tag{16}$$

Here D_s is obtained from Rishbeth and Edwards (1989). R is the universal gas constant. T_i and T_e are ion and electron temperatures, respectively. During night time, it is assumed that $T_i = T_e = T_n$.

$$K_1 = 0.93 * \left(\frac{T_n}{1000}\right)^{0.37} * 10^{-16}\ \mathrm{m^3\ s^{-1}} \tag{17}$$

$$K_2 = 3.9 * 10^{-16}\ \mathrm{m^3\ s^{-1}} \tag{18}$$

Here K_1 and K_2 are obtained from Gurubaran and Sridharan (1993).

As time elapses, electric field/neutral wind can cause vertical drift of ionization and in effect, it will result in the indulgence of vertical ionization drift due to these two factors too. Thus, in the presence of electric fields and neutral winds, the above case will be governed by the servo equation by Rishbeth et al. (1978). i.e., the peak height h_m will approach exponentially towards the non zero drift equilibrium level at a rate determined by diffusion and loss in the stationary level.i.e., Hence the SERVO equation is given as:

$$V_p = H\left[\frac{dZ_m}{dt} + \frac{D_s \sin^2(I)}{2H^2}\left(e^{Z_m} - e^{-kZ_m}\right)\right] \tag{19}$$

Here Z_m is the reduced height of F2 peak height, V_p is the vertical plasma drift. In the presence of electric fields/neutral winds, V_p can be also written as,

$$V_p = V_E \cos(I) + U_m \cos(I)\sin(I) \tag{20}$$

Here $V_p \sim V_H$ and V_E is the component of ion drift velocity perpendicular to the Earth's magnetic field. It is obtained as the ratio of eastward electric field, E and magnetic field, B. i.e.,

$$V_E = \frac{E}{B} = \frac{d(hpF2)}{dt} - \beta H \tag{21}$$

Here $V_E \sim V_T$, since electric fields are important in the equatorial regions.

By equating (19) and (20), meridional neutral wind U_m can be obtained. i.e.,

$$U_m = \frac{dZ_m}{dt}\frac{H}{cos(I)sin(I)} - \frac{D_s sin(I)}{2Hcos(I)}\left(e^{-kZ_m} - e^{Z_m}\right) - \frac{\frac{E}{B}}{sin(I)} \tag{22}$$

Previously mentioned two ionosonde stations are employed in this method too for obtaining hpF2 values. $\frac{dZ_m}{dt}$ in the Eq. (22) is calculated at every 10 min interval, where the reduced height, Z_m is obtained by,

$$Z_m = \frac{(hpF2 - h_s)}{H} \tag{23}$$

In Eq. (22), hpF2 is referring to the one at low latitude station. H refers to the Atomic Oxygen scale height given by Fagundes et al. (1997) $H = 0.058 * T_n$, T_n is the neutral temperature at hpF2 height which can be obtained from MSISE 90 model. The values of h_s are obtained at each heights from 100–750 km and this occur at the point where left hand side and right hand side of the balance equation given in the Eq. (13). As mentioned in the previous method, in the above expressions also, the neutral temperature T_n and neutral number densities of N_2, O_2 and O^+ are obtained from MSISE 90 model.

2.3. HWM07 Model-the empirical model for meridional winds

HWM07 is an empirical model which provides the horizontal neutral wind in the upper thermosphere (Hedin et al., 1991). The model uses wind data from AE-E and DE 2 satellites and provides the zonal and meridional winds for the latitude, longitude time and Ap index specified. In this study, we have attempted to compare the results of winds estimated using h'F and hpF2 methods with the HWM07 model winds for the equinoctial months.

2.4. Superposed Epoch Analysis (SEA) method

Superposed Epoch Analysis is a powerful tool which consists of sorting data into different categories and comparing means for them. The process can be also termed as compositing. The main principle is that on averaging the data in a proper way in relation to the event. The event signal will retain and all other influences will undergo averaging. i.e.,in brief, we can say that the data sequence can be broken to different sets of equal duration and all the sets can be made to superpose. Execution of the SEA technique involves several steps. As a first step, the data is categorized with equal durations and then mean of each section is obtained. Thus for a sufficient data, common response to an event should emerge in the form of average, while noise in the data will be cancelled out. Superposed Epoch Analysis has been a very useful technique commonly used for identifying the behaviour of geomagnetic storms.

In the present study, for each ESF event, we divide the category of both meridional wind and h'F into ten minute duration (since time resolution is ten min) prior to and after 1hour of the ESF onset. The ESF onset on each day is considered as '0'. Then, 1 h prior to and after the onset has been considered. Therefore, estimated wind and h'F values are categorized into an hour before and after the ESF onset including the onset. Hence in this case, a total of 13 classifications will be emerging and for all the ESF days. Finally, once these categorization is done, the mean of each category is obtained and this averaged value under each category will be shown in the figures. Hence this analysis helps to understand h'F and wind variations within that particular period of ESF onset, before an hour and after an hour to the onset. This analysis is useful in analyzing the meridional wind and h'F variations around the time of ESF onset and can be valuable in evaluating the plausible importance of each parameter contributing to ESF generation. Here for March case, since h'F and wind values are of twenty minute resolution, we will have −60,-40,-20 etc epochs defining the 1 h prior interval of ESF event. The ESF onset is taken to be as Zero. Similarly, one hour after the ESF onset is taken as +20, +40, +60 etc.

2.5. GPS scintillation data

Often, electron density irregularities in the ionospheric region results in degradation of the radio wave signals causing fluctuations in amplitude and phase of the signal received at the receiver. In order to measure the amplitude scintillations, S4 index is a widely used parameter which is obtained as the normalized standard deviation of the intensity of the received signal power. In our study, we concentrate on the GPS L band (L1 frequency at 1.57542 GHz) amplitude scintillation data and from the S4 index and scintillation duration. Only those events were considered as scintillation days whose duration is above 0.5 h, while duration lesser than this value are considered as non scintillation days. Since the period under study is equinoctial months, we have majority of them as scintillation days, while a few are obtained as non scintillation days.

3. Observations and results

3.1. Estimation of night time meridional winds using h'F method-some case studies

Present section describes the observations and results of the study in detail. Fig. 2(a) shows the h'F, vertical drift and wind variation for March 13–14, 2013 a spread F day, which is quiet (Ap value = 3). The blue and red horizontal bars in the upper panel of the figure indicates the spread F duration over TIR and HYD respectively. The bottom panel shows the h'F values at TIR and HYD in blue and red colour curves respectively, the middle panel gives the vertical drift, dh'F/dt for both stations. Top panel gives meridional winds estimated over HYD as derived from h'F data at the two stations (TIR and HYD), by including necessary corrections for plasma diffusion and chemical recombination. The spread F over TIR started at 19:20LT and continued till 02:00LT over TIR. Poleward wind decays since 18:00LT, reaching its lowest value at 19:20LT and reaching an equatorward value of about −50 m/s at 20:45LT. h'F at TIR was at 300 km by 18:50LT, which thereafter starts increasing and reaches a maximum of 410 km at 19:30LT. Spread F at HYD occured at 19:40LT and lasted till 5:00LT. We can notice that h'F at HYD has not reached beyond 300 km. A descent in the h'F at both stations are visible after 00:00LT. Correspondingly, there is no poleward reversal of winds. The meridional wind after reaching the equatorward peak at 21:00LT, reverses to poleward and stays there till 22:30LT. Afterwards, it was seen to remain in equatorward direction with a comparatively more equatorward value of −150 m/s around 00:00LT. This equatorward sustenance of wind lasted for 5 h.

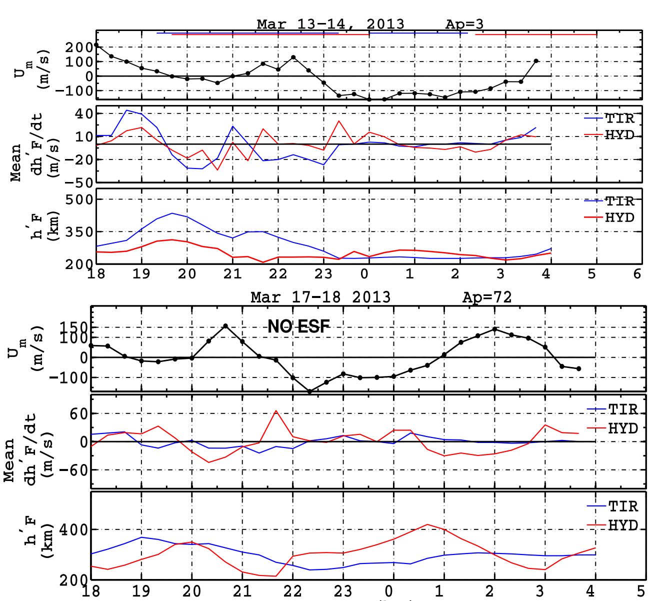

Fig. 2. (a) A case study showing the variation of h'F (bottom panel), dh'F/dt (middle panel) and the meridional wind (top panel) for March 13–14, 2013 (Ap = 3, Quiet day, Spread F day); (b) for March 17–18(Ap = 72, disturbed day, Non Spread F day).

Fig. 2(b) shows the h'F, vertical drift and wind variation for March 17–18, 2013, a non spread F day, which is a disturbed day too (Ap = 72). Out of the days analyzed, this was the only day with non occurence of ESF in March. It can be noticed that the poleward winds decreased and reached equatorward by 19:00LT associating which the h'F crossed 350 km. It is important to note that here spread F is absent over both stations. In this particular case, absence of spread F can be due to the effect of geomagnetic activity. Around 19:00LT, the h'F value at TIR is well above 300 km, where as HYD h'F level is lesser than that. The drift values are nearly 20 m/s for both stations. Though the wind turned equatorward sligtly by 19:00LT, no spread F is observed in both stations. Since this day being a highly disturbed day too, it is difficult to differentiate the effects of wind and geomagnetic activity influence. But larger poleward wind amplitude of about 150 m/s is seen by 20:00LT and equatorward magnitude of the order of 160 m/s are observed by 22:10LT. At 22:20LT, wind reversed back to poleward direction with maximum value of 150 m/s occurring at 2:00LT and thereafter a reversal to poleward again. It is obvious that this day, in comparison with spread F day showed larger poleward wind magnitudes before and after midnight. The decrease in h'F values at HYD are evident at the time of poleward reversal of meridional winds.

Fig. 3(a) shows the meridional winds estimated during April 21–22, 2013, an ESF day with Ap = 2. The poleward wind magnitudes seems to be increasing since 18:00LT till 20:10LT. Its decay (equatorward turning) started by 20:20LT. While considering the case of h'F, it has reached 300 km at 18:50LT and a maximum of 410Km at 20:50LT. The Spread F over TIR started by 20:40LT, existed till

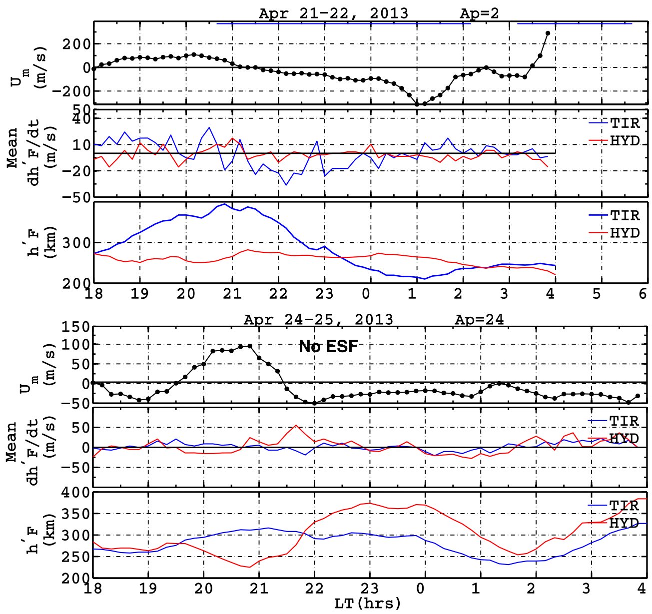

Fig. 3. (a) A case study showing the variation of h'F (bottom panel) dh'F/dt (middle panel) and the meridional wind (top panel) for April 21–22, 2013 (Ap = 2, Quiet day, spread F day); (b) for April24–25, 2013 (Ap = 24, disturbed day, Non spread F day).

2:10LT and continued after a break of one hour till 05:30LT. HYD station didnot show spread F. h'F at HYD around the period is seen to be well below 300 km. It is clear that once the wind starts turning equatorward, it consequently raised h'F and this might have contributed to the onset of ESF on this day. The corresponding vertical drift was 25 m/s. From 21:00LT to 01:00LT, it remained equatorward. Equatorward peak was reached at 01:00LT with a magnitude >200 m/s. Poleward reversal occured around 01:00LT, but its magnitude remained within negative values. This equatorward values remained till 03:30LT afterwards, it took a clear poleward turn. The F layer descent at HYD is observed from h'F values in association with poleward reversal of the wind.

Fig. 3(b) shows a non ESF day of April 24–25, 2013, a disturbed day, with Ap = 24. In this case, unlike previous non ESF DAY, the h'F values at both TIR and HYD remained well below the level of 300 km. After 20:30 LT only, TIR h'F values increased beyond 300 km. While the meridional wind values were equatorward till 19:00LT, afterwards it reduced in magnitude and reached the maximum poleward magnitude of 190 m/s by 21:00LT. This behaviour of the meridional wind seems to be similar with the previous case study of non ESF day. After 22:00LT, wind remained equatorward throughout the night, though there is a slight poleward reversal (reduction in equatorward values) by 01:00LT which is associated with this reduction, F layer descent is seen in h'F values of HYD as well as TIR and this behaviour is quite different from the case of disturbed day on March.

While the above case studies show the h'f and wind variations during Equinoctial months, it will be interesting to look into wind variations of the Summer month. With regard to this, we have analyzed the h'F data for May 2013 too. Fig. 4(a) is a case study on May 23–24, 2013 with Ap = 8. The meridional winds showed a double peak structure in this case. Poleward wind values started to decrease from 19:30LT onwards. h'F values were above 300 km after 19:00LT and its peak (350 km) reached by 20:00LT only. The wind reached equatorward by 21:30LT. Vertical drift values are 30 m/s for TIR at the instant. The spread F at TIR started at 19:40LT and remained till 23:50LT. Spread F is seen at HYD from 02:00LT onwards which sustained 3 h. At 23:30LT, wind became equatorward completely with a maximum value of 159 m/s, afterwards its direction reverses at 00:00LT. After 01:00LT, again the wind remained equatorward only. It is clearly seen that the wind pattern in May is different from equinoctial months with a sustained equatorward velocity in the post midnight period. HYD station is having an increase in h'F values thereafter when compared to TIR h'F values.

Fig. 4(b) is for May 15–16, 2013, a non spread F day (Ap = 8). Here till 20:00LT, h'F at TIR remained less than 300 km, until 19:50LT. From 18:20 to 19:30LT, wind was poleward, after a slight decrease in poleward magnitude, it again increased and remained till 21:00LT. The h'F at TIR just reached 300 km. h'F at HYD was below 300 km. After 21:30LT, the poleward wind reversed to equatorward and sustained as it is till 03:00LT, afterwards it gained strength in poleward direction. It is also seen that well associated with the poleward reversal is seen the F layer descent in HYD. The two cases in May thus showed a consistent trend of sustained equatorward winds till 03:00LT. Also, it can be noticed that the MTM effect,

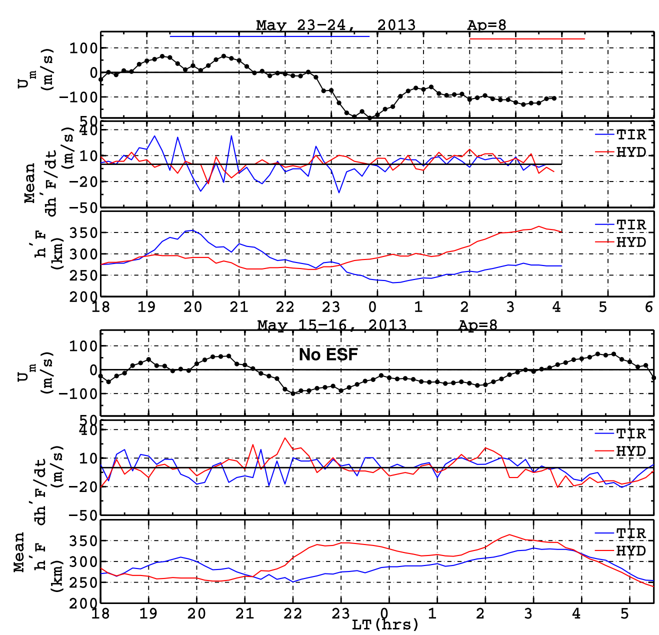

Fig. 4. (a) A case study showing the variation of h'F (bottom panel) dh'F/dt (middle panel) and the meridional wind (top panel) for May 23–24, 2013 (Ap = 8, Quiet day, spread F day); (b) for May 15–16 (Ap = 8, Non spread F day).

i.e., the poleward reversal of winds after midnight is not present or even if it is there it shows a delayed effect.

3.2. Comparison of meridional winds derived using h'F values with hpF2 values (SERVO method) and HWM07 model

Fig. 5(a) and (b) depicts the comparison of two methods and the HWM07 model for March and April 2013 for the quiet ESF days respectively. The bottom panel gives the winds estimated from h'f values; middle one is for hpF2 values and top one shows the HWM07 winds. In the bottom panel, light blue curves show 15 days for which winds are estimated, with mean wind in black colour and corresponding standard deviation is also included. Middle and top panels also follows the same, except for mean winds and standard deviation are plotted in red colour and dark blue colour respectively. During March, mean wind for h'F method clearly shows a decreasing poleward pattern till 20:00LT. Afterwards, a slight increase in poleward direction is seen till 21:40LT, with a reversal to equatorward. Between 23:00LT and 24:00LT, a clear poleward reversal is seen in the figure. While in the hpF2 method, though winds are equatorward before 22:00LT, it increases to poleward afterwards. As expected, the HWM wind variations are comparatively smoother, in such a way that a reduction in poleward magnitude and hence followed by an equatorward peak at 24:00LT, which afterwards undergo a poleward reversal similar to the h'F method. Although HWM wind values are lower than the derived wind values, it is evident that h'F method shows similarity to HWM07 model winds in comparing them. The equatorward peak in the early night hours and poleward peak in the post midnight hours are slightly delayed for hpF2 derived winds, where as the peaks are almost matching in other two methods. Further the standard deviations associated with the HWM07 model is lesser than other two methods. On comparing hpF2 derived winds, h'F winds seems to have lesser standard deviation.

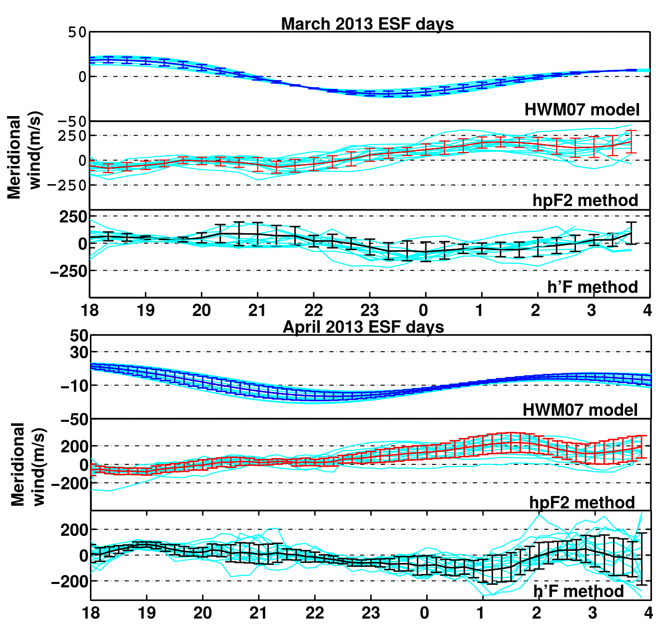

Fig. 5. Comparison of the meridional winds derived using h'F and hpF2 data along with HWM07 model for the two equinoctial months (a) March and (b) April 2013, the mean wind and standard deviation is shown in black, red and blue colour respectively. (For interpretation of the references to colour in this figure caption, the reader is referred to the web version of this article.)

During April, it is seen that the mean meridional wind derived from h'F values are directed poleward in the early evening hours from 18:00LT to 19:00LT. Further, poleward wind magnitude is reduced until 21:30LT. An equatorward turning clearly occurs both in magnitude and direction by 22:00LT. After the midnight, a clear poleward reversal of the wind occurs at 01:00LT with a poleward peak near 03:00LT. hpF2 derived winds have an equatorward peak in the pre midnight hours at 19:00LT. Thereafter they exhibit a poleward pattern only unlike the HWM and h'F derived winds. h'F derived winds have an equatorward peak 23:30LT, thereafter which follows a poleward direction with peak around 02:30LT which almost coincides with HWM model winds. Thus in general, it can be seen that h'F derived winds through their directions are consistent well with HWM07 model winds.

At this point, we would like to discuss qualitatively about the errors that could have come in the meridional wind estimations. Since scaling of ionograms during spread F is tedious task, extreme care has been taken in the same. Still, there is scope of error which can be due to error in scaling hpF2 variations as well as h'F during spread F times. Hence uncertainities in h'F can affect the vertical drift terms. During spread F times, the uncertainity in h'F can go up to ±15–20 m/s and this can lead to an uncertainity in the estimated meridional winds to be ∼±40–50 m/s. Although the h'F data method and hpF2 method are carried out at different altitudes, due to the reason that there are not much effect of vertical gradients in these winds, there would not be much differences in both methods in regard to this. Further, the neutral temperature and densities obtained from MSISE 90 model also can bring in some part of errors which we have not calculated separately. Gurubaran and Sridharan (1993) suggested that differences can exist in the spectroscopically determined neutral temperatures and temperatures obtained using MSISE-90 model, which thereby can alter the measured wind values. Since these thermospheric neutral parameters are involved in the ion-neutral collision frequency and loss coefficient terms (parameter T_n, through K1 and K2 terms and directly through neutral densities of N_2 and O_2) there by producing uncertainities in them and correspondingly in estimated wind values.

Using hpF2 data method, the main possible error source can be uncertainities in hpF2 and h_s and hence there can be differences in the reduced height term, Z_m. This non linear terms are absent in h'F method. Scaling errors in hpF2 during spread F times can cause uncertainities in these terms. Further the errors in h_s could arise from the balance equation which involves some of the important terms like D_s and βs. We know that these terms further include parameters like neutral temperature and densities which are obtained from MSISE 90. In addition to that, uncertainities in Tn can lead to differences in K1 and K2 as well as in Atomic Oxygen scale height terms. Another important difference factor for winds estimated using both methods include the presence of the terms e^{z} and e^{-kz} which denotes the time constants due to ionization loss and recombination effects. It is clear that these constants differ with height and they are included in the method using hpF2 and omitted in h'F one. This extra term may cause further variations in winds estimated using hpF2 data.

During a comparative study using the methods by h'F and hpF2 datas in the Brazilian sector, Muella et al. (2008) showed that during spread F days, meridional winds calculated from hpF2 data may lead to errors of about 59 m/s, while those with h'F may produce errors of about 69 m/s. Also, they suggest that winds estimated for h'F method was calculated over a station with dip angle of 32°, where the effects of electric field are not much important when compared to effects of other factors like meridional wind, diffusion etc. Present study is carried out at a more near equatorial station with dip angle 23°. This might give comparatively better winds values using h'F data.

Thus overall, it can be seen that the number of input parameters used in the wind estimations using hpF2 data is comparatively larger than those using h'F method. This might be the reason by which we could see a better agreement of winds estimated from h'F data rather than hpF2 data.

Fig. 6 indicates the mean value of winds during May, 2013 which is given in dark blue colour along with their standard deviation. Here, mean winds are calculated for h'F method only. The wind magnitudes are comparatively lesser during the May season. Most of the days showed a consistent feature of equatorward wind especially in the post midnight sections. During 18:00LT–19:10LT, the winds are clearly poleward with a maximum value of mean wind reaching about 50 m/s. After 19:10LT, poleward velocity reduced and continued until 21:00LT. This was followed by equatorward turning, with equatorward maximum being −50 m/s at 23:10LT. Thereafter, the equatorward values reduced, still within the equatorward polarity values-a striking feature observed in majority of cases analyzed in the month of May. Here the poleward reversal is not evident.

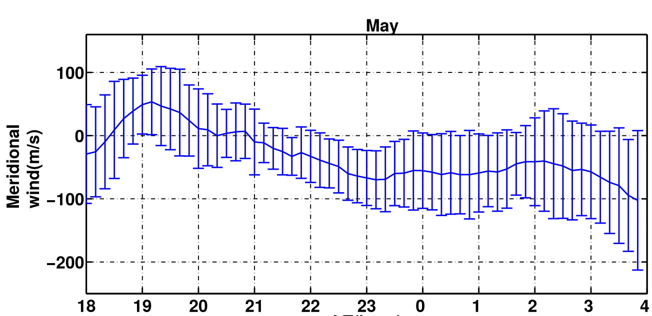

Fig. 6. h'F method plot for May is given along with the mean wind and standard deviation.

3.3. Superposed Epoch Analysis study of h'F and meridional winds during the equinoctial period

In this section of SEA technique, winds derived from h'F method has been used. Method of superposing has been described in the data and methods section. The bottom panel in Fig. 7(a) represents the superposed wind values for March, where as top panel of the same refer to corresponding h'F values. From the figures, we can infer that at zero epoch, i.e., at ESF onset the wind poleward wind values are beginning to reduce, though it is not reaching completely equatorward (negative) values. At the same epoch (at ESF onset), h'F almost reaches a maximum. Although a clear maximum occurs ten minutes after that. In the case of meridional wind, larger scales makes the slight poleward reduction to be hardly visible. This slight reduction in the poleward wind magnitude occurs for approximately 40 min. Afterwards an increase in poleward direction takes place. Regarding h'F values, they reach a mean value of peak at approximately 390 km. Although just before that, meridional wind turns slightly poleward, but its effect doesn't seem to be affecting much. Fig. 7(b) shows the same exercise done for April months. The April month is having a better resolution of 10 min. Rest of the description remains the same. It can be seen that h'F peak time was similar in March as well as April months, whereas, in April month a clear reduction in the poleward magnitude is visible since 30 min prior to ESF onset which

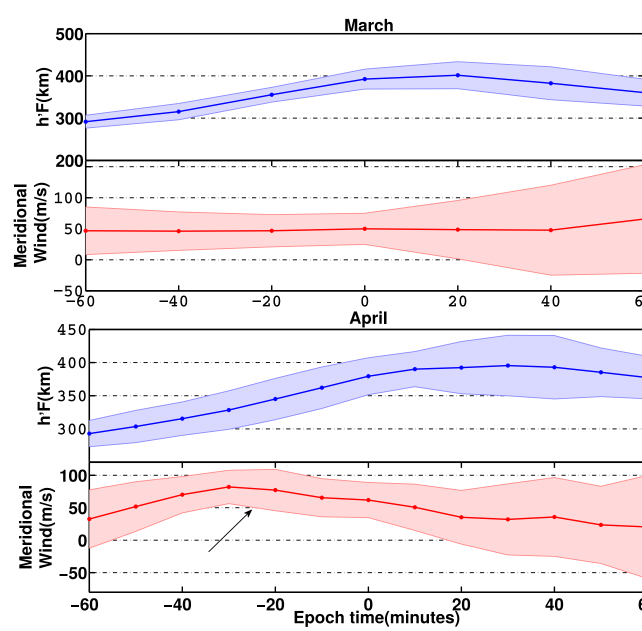

Fig. 7. Superposed Epoch Analysis applied (SEA) for the h'F and meridional winds during (a) March and (b) April 2013. Here the time interval of one hour before and after the ESF onset has been considered. Standard deviations are also shown in the corresponding plots.

afterwards also undergone further reduction till an hour after ESF onset. Considering h'F values, it can be seen that the mean value of the peak h'F reaches as high as 440 km. In this month, it is clear that the equatorward reversal (reduction in poleward magnitudes) suggests their assistance in raising the h'F values to higher levels. Thus the application of this technique can bring in general pattern of thermospheric meridional winds as well as h'F.

3.4. h'F vs meridional winds for ESF/GPS scintillation events

Fig. 8 represents the h'F vs meridional wind values for March and April months, taken just before ESF onset. In the present study, we consider the polarity of the winds just before the onset of ESF in the ionograms and not later than that and hence the corresponding uncertainties are at their minimum. We have divided the ESF duration into 4–8 h and 9–12 h which is represented by blue and red dots respectively. As in our study there are only two points which fell under equatorward (−ve) polarity, but here we still consider wind values up to 50 m/s as lesser poleward magnitude which can affect the height rise and consequently ESF. It is seen that just before ESF onset, lesser duration events have meridional wind values in highly poleward directions mainly. For longer durations, meridional wind values range from equatorward to poleward wind values. Apart from that, if we observe keenly without separating on the basis of duration of events (only h'F vs wind values), another interesting pattern also emerges, i.e., as the poleward wind magnitudes increases, h'F at TIR can be seen reducing, although there exists some outliers.

Fig. 9(a) represents h'F vs meridional wind values for March and April 2013 which is further classified on the basis of presence/absence of scintillations. In this case, only those events were considered whose duration is above 0.5 h. The events with GPS scintillations present over TIR is denoted by red dots, whereas the absence of GPS scintillations is shown in blue dots. Although the number

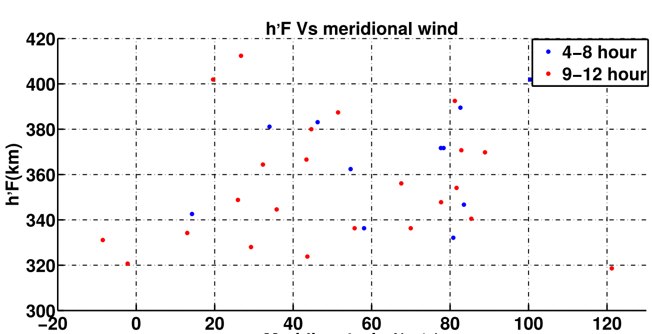

Fig. 8. Scatter plot of the meridional wind values vs h'F values at TIR just before ESF onset corresponding to each of the ESF cases of March and April, 2013. Blue points correspond to the events with 4-8 h ESF duration whereas red denotes the events with 9–12 h duration. (For interpretation of the references to colour in this figure caption, the reader is referred to the web version of this article.)

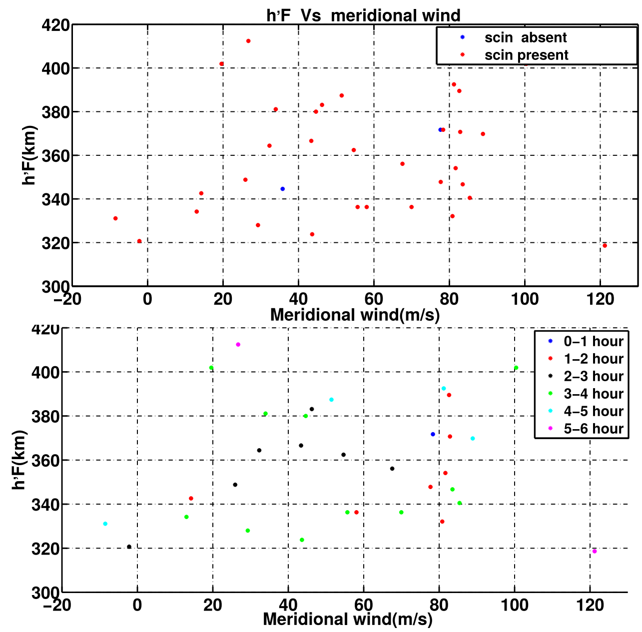

Fig. 9. (a) Scatter plot of the meridional wind values vs h'F values at TIR just before ESF onset corresponding to each of the ESF cases of March–April, 2013. Blue dots correspond to the events on the days scintillation was absent, whereas red dots denotes the days scintillation was present. (b) same as in panel(a), but classified on the basis of duration of scintillation. (For interpretation of the references to colour in this figure caption, the reader is referred to the web version of this article.)

of scintillation days are limited to two only, a clear separation is seen such that during the absence of scintillations, just before the ESF onset, winds are poleward in direction. At the same time, in the case of GPS Scintillation present, wind values range from equatorward to poleward directions.

Fig. 9(b) classifies the h'F vs wind values in terms of 1 h duration each for GPS scintillation days. Corresponding colour legends are shown in the figure for each classification of duration. Unlike the previous cases, this particular classification doesnot show a clear cut result, but careful observation shows that the lesser duration scintillation events are more concentrated on the higher poleward magnitudes. Similarly, as the scintillation duration increases, poleward magnitude reduces or it even reaches the equatorward values. Upon reclassifying them into groups with scintillation duration of 0–1, 1–2 and 2–3 h duration and another section into 3–4, 4–5 and 5–6 h duration, the same trend remains. i.e., the first section events are more concentrated only on the poleward magnitudes. The second section events seems to range from equatorward to poleward magnitudes. Although in both cases, a few points deviate from this behaviour, the majority go in hand with this pattern.

3.5. Meridional winds variations on scintillation vs non scintillation days

Fig. 10 shows the mean wind variation on scintillation vs non scintillation days of March 2013. Month of April was not having any scintillation events according to the criteria we applied (mentioned before). The winds on scintillation days are represented by blue curves, while those on non scintillation days are given by red curves. Corresponding standard deviation are also shown for further clarity. On scintillation days, the meridional winds are having clear reduction in poleward magnitudes, until 20:00LT. Then on, a slight increase is visible for an hour. Later on, at 22:00LT, the wind turns equatorward and reaches a peak of −98 m/s at approximately 23:30LT. At 00:00LT, equatorward wind reverses to poleward direction. On non scintillation days, it is obvious that wind is poleward for the time duration of 18:00–21:00LT. Upon reaching a maximum amplitude of approximately 120 m/s, it reverses to equatorward direction at 21:30LT. Finally, the maximum equatorward peak of 190 m/s is obtained at 00:30LT followed by a poleward reversal. Comparison between the scintillation vs non scintillation days indicates clearly opposite pattern during the early night hours. Similarly, the equatorward reversal of winds occurs earlier for scintillation mean winds than non scintillation days. Hence, equatorward peak is reached an hour early for scintillation case. Correspondingly, poleward reversal occured earlier for scintillation days than non scintillation days. Also, equatorward peak value for non scintillation days is larger than non scintillation mean wind.

4. Discussions

Present section includes a brief discussion of overall results obtained in the study. Day to day studies reveal the variation in wind pattern in association with ESF. First case of ESF day in March clearly shows an equatorward trend of winds (reducing poleward magnitudes) just before ESF onset, though the reduction starts from 18:00LT onwards. In this case, h'F was already well above 300 km. We are well aware that, the equatorward winds have the ability to raise the h'F height levels. Biondi et al. (1988) showed the night time meridional winds at 300 km which was equatorward most of the time. The

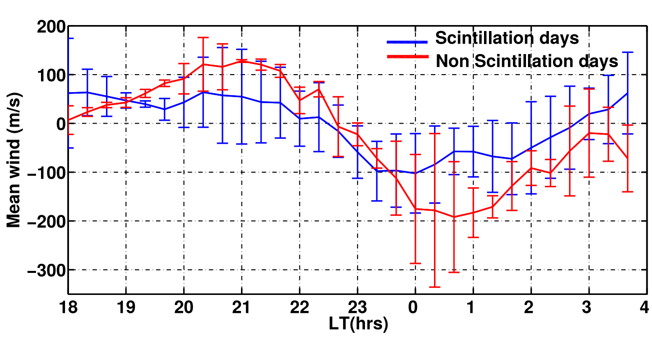

Fig. 10. Mean wind vs time for scintillation vs non scintillation days in March 2013 is shown. Blue curve denotes the scintillation days and red denotes the non scintillation days. (For interpretation of the references to colour in this figure caption, the reader is referred to the web version of this article.)

observation was made at Arequipa (geographic latitude 16.3°S, longitude 72.5°W) using airglow measurements with Fabry Perot Interferometry technique (FPI). The role of PRE in causing the increase in height of F region is also a major part in the post sunset F region over TIR. Though the h'F was at 300 km by 18LT, it will be suitable to suspect that the reducing poleward winds might have a positive influence on the F layer. In this particular case, it is evident that both h'F through PRE development and equatorward winds further assisting in raising it could be playing a compromising role in the ESF generation. RT instability is the main factor for the initiation of ESF with sufficient background conditions. i.e., Once the F layer is taken to higher altitudes above a critical level, RT instability starts operating. Here it can be assumed that in addition to PRE developed from F region dynamo process, the equatorward wind might have further assisted the increase in h'F. The presence of larger PRE effect and corresponding increase in the height might have involved in the occurence of spread F in the off equatorial station, HYD. The analysis of the non ESF day revealed the presence of large poleward winds around the usual ESF onset time. Although an equatorward wind motion is seen prior to that, the poleward surge of nearly 150 m/s was so sudden that it might have prevented the ESF generation. It is to be noted that the poleward turning of the wind was delayed in the earlier event. Further, the absence of ESF might be also due to the increased geomagnetic activity.

Another example in April shows a poleward pattern which starts to reduce before the ESF onset. The spread F is delayed by an hour compared to the previous ESF day. Though the layer was well above 300 km, ESF at TIR did not started suddenly, instead it started only after the poleward wind started to reduce in magnitude. This is a furthermore clear case of the wind effect which is more dominant than assisting the h'F values. The large poleward winds of approximately 110 m/s might have suppressed the spread F occurence in HYD. Further, the lower E X B drift and hence lower h'F values over TIR might have also had a contribution in the absence of ESF over HYD. This can be in accordance with the results of Abdu et al. (2006) and Maruyama (1988) where they suggest that large poleward winds can result in causing an asymmetric ionization anomaly and subsequent increase of Flux Tube integrated conductivity and hence a reduction in RT instability growth rate and further inhibiting vertical growth of the bubble. This controls/limits the latitudinal coverage of plasma irregularities. Considering the non ESF day example in the month, a large poleward wind of 160 m/s was initialized before 19:00LT. Correspondingly, the h'F values are well below the threshold level mentioned by Devasia et al. (2002). It points to the fact of a probably weaker F region dynamo. Further the large poleward polarity of wind might have further suppressed the h'F values. As a preliminary observation, we suspect that this poleward wind could have reduced the chances of non occurence of ESF. As pointed in the previous example, one has to be cautious about the increased geomagnetic activity effect too.

Other than equinoctial months discussed, analysis during May reveals a quite different nature of meridional winds. The first difference noted being the reduction in meridional wind amplitudes than the other months considered here. Although during 18–19:30LT, a predominant poleward wind was present, the lesser magnitude of it and subsequent turn to equatorward direction might have indulged in assisting the h'F. A reduction in the poleward magnitudes by 19:30LT marks the ESF onset for this season as well. After 22:00LT, the wind direction turned equatorward and remained equatorward for the post midnight hours. The non ESF occurence on HYD indicates that the poleward magnitude of the wind was comparatively lesser which might have negatively influenced the latitudinal extension. Non ESF event example of May shows a double peak in poleward direction in the early sunset hours. Being a quiet day, it is easier than previous cases to verify the effect of meridional wind. h'F lies below 300 km around 19:00LT. The poleward wind might have reduced the further increase of h'F, which is already under the action of a weak PRE. It seems that the enhanced poleward wind could have caused the reduction in PRE. The variability in the wind pattern could be attributed to the variation in the upward propagating semi diurnal tides.

In the post midnight period of both March–April seasons, there is a clear poleward reversal in wind seen in between around 00:00–01:00LT which might indicate the existence of Midnight Temperature Maximum. Using satellite data, first in situ measurement of MTM was made by Spencer et al. (1979) and reported that near local midnight, there exists a recurrent neutral temperature enhancement accompanied by a poleward surge in the meridional winds. By making use of airglow emissions studied from the All sky imager at Arequipa, Colerico et al. (1996) made the first ground based MTM observations. They observed this particular MTM signature as enhanced $6300A^{o}$ airglow which apparently propagated from northeast to southwest near local midnight. The role of MTM as a cause for the post midnight poleward reversal of equatorward winds has been discussed in some works over the Indian sector (Sastri et al., 1994) in which they mention the midnight collapse of F layer in association with poleward reversals of neutral winds. Non ESF days for different seasons were studied by Hari and Murthy (1995) and they concluded that the stronger MTM at equinoxes are responsible for the stronger poleward reversal of the winds during equinoxes. Thus the present study is in agreement with their result and further, our results may be thus indirectly confirmed. However, based on a study from the hmF2 derived meridional winds from Cachoeira Paulista, Batista et al. (1997) suggested that MTM related effects on neutral winds were not visible during equinoxes. The reversal of equatorward to poleward wind-signature of MTM is not visible in the month of May and instead winds were predominantly equatorward.

The comparison of winds derived using h'F values has been carried out with hpF2 values (SERVO method) and HWM07 model which reveals varying agreements as well as disagreements. Both the equinoctial months clearly shows a better agreement of h'F derived winds and HWM07 model winds when compared to hpF2 derived meridional winds. According to Murthy et al. (1990), the error associated with the meridional wind on a non ESF day would be ±25 m/s. For a spread F day, it can reach up to ±40–50 m/s, since the uncertainty in the determination of h'F would be ±15–20 km. Present study obtains the standard deviation of the meridional wind, it is obvious that around spread F periods, error is slightly more. The standard error is minimum for HWM derived winds. This is in accordance with previous reports. Further the peaks in the h'F wind was having good similarity with HWM07-model. This is well noticed in the time of poleward wind peak in between 02:00 and 03:00LT for both h'F and HWM07 winds. It has been reported by Muella et al. (2008) that h'F method works better for equinoctial periods due to not so high values of winds during equinoxes leading to higher values of F region heights. However, their work explains the winds estimated using a station of dip angle 32°, whereas in the present study the winds were estimated using a low latitude station with dip angle 23.53°. This could have lead to the comparatively better wind values using h'F data.

Hence, in our study, considering that h'F method works better in comparison with other methods, we proceed to understand how the meridional winds can affect/control the ESF. The Superposed Epoch Analysis of meridional winds and h'F during ESF days are obtained so as to understand the general behaviour of winds an hour before and after ESF onset which is a unique part of this study. Using ground-based experimental data from the northern hemisphere, works have been done using the method of superposed epoch with an aim to investigate the influence of geomagnetic disturbances on the wind field between about 70 and 100 km. A better picture of the Superposed Epoch Analysis is obtained from the meridional winds estimated in the month of April. It is to be noticed that before 30 min of ESF onset, the winds started reducing its poleward magnitude, at the same time the h'F was well beyond a threshold level of 320 km. The same figure for March season meridional winds do not show a prominent reduction in poleward winds as compared to the April ones, whereas h'F values shows a similar behaviour to that of previous case. However, by the time of ESF onset, winds started slightly to reduce their poleward magnitudes which is not so prominent as the April case. The important finding from this particular method carried out on ESF days is that the general behaviour of the winds and h'F is such that both are equally contributing to the ESF generation process. It appears that reduced poleward wind magnitudes (turning to equatorward wind) has a positive influence on RT instability growth rate and hence ESF occurence.

The long duration ESF/scintillation events can have a tremendous impact on communication systems. In that regard, knowledge of the factors contributing to it can be also useful. Not many works have carried out on the polarity/magnitude of meridional wind before ESF onset and how they contribute to ESF duration. h'F vs meridional wind velocity has been plotted in terms of ESF Duration of 4-8 h (lesser duration) and 9–12 h (long duration) at TIR. This particular classification enables to see how the behaviour of wind affects the duration of ESF. Sreeja et al. (2009) have studied the variation of the duration of ESF during different geophysical conditions and they reported that the estimation of the duration of ESF on a day can be done by using geomagnetic Kp index and post sunset vertical drift. In our study, we attempt to analyze the importance of meridional wind before ESF onset in the ESF duration. The main finding here is that majority of the points for which ESF duration of 4-8 h (red dots) are seen in the poleward magnitude, while the points for which ESF duration of 9–12 h (blue dots) are concentrated in the lesser poleward magnitudes as well as two points are coming in the equatorward wind magnitudes. This concludes that duration of ESF could be affected by the magnitude of poleward/equatorward winds. The figure also gives a clue about the relation between h'F at TIR and meridional winds. Considering threshold height as a parameter controlling the ESF day to day variability, Devasia et al. (2002) reported that the ESF occurence pattern can be modulated by converging/diverging meridional winds, mainly equatorward wind have a significance when h'F is below the threshold height for triggering RT instability. They studied the need of a threshold height of 300 km, below which equatorward plays an assisting role. Here, as a matter of fact, due to lesser number of equatorward wind points, we don't fix a particular threshold height. However,one on keen observation can suggest a threshold height of 320 km (in this study). Here, it can be reminded that threshold height below which equatorward wind come into picture can be varied according to solar flux values. We have obtained a positive correlation of h'F just before ESF onset with solar flux values (not shown here). According to solar flux values over the two months, it seems that it is well correlating with the figures of moderate to high solar flux values shown in Fig. 2 of Jyoti et al. (2004). However, the present case is lacking more number of equatorward winds. Thus it can be suggested that under the post sunset electrodynamic drifts, the combined effect of higher base heights and lower poleward winds might be contributing to the ESF generation.

The figure also reveals a special kind of pattern for duration of ESF and wind magnitudes. Keen observations point out that longer duration events are bounded by equatorward to poleward values, especially if we are considering a threshold for wind magnitudes approximately nearby 60 m/s, it is clear that majority of the long duration events fall below this category. i.e., other than the two points which are clearly equatorward, poleward magnitudes of lesser values also seems to have a part in having the long duration ones. In the case of short duration spread F events, we can see no points are coming in the equatorward magnitude region, instead they follow a trend such that lesser poleward magnitudes to higher poleward values. Again, a threshold of 60 m/s if assumed from the figure, it is easily observed that majority of the points for shorter duration events can be categorized as residing above 60 m/s, which can be considered as higher poleward magnitudes. In this process, we tend to omit some outliers which are visible in the figure. Thus on a broad way a relation of meridional winds to ESF duration can be obtained, which to our knowledge is not presented earlier.

It is well known that L-band scintillation occurrence is largely controlled by the EPB occurrence. So the factors which contribute to ESF day to day variabilities can directly/indirectly affect scintillations too. When considering the case of L-band scintillations, the presence/absence of scintillations has been tried to analyze using h'F Vs meridional wind values which clearly indicates that the events where GPS scintillation were absent are concentrated in the poleward magnitudes. The presence of GPS scintillations and winds are such that they spread from equatorward to poleward magnitude range. This study has been limited to lesser number of non scintillation events since equinoxes months are being studied. A similar kind of classification as in the case of ESF cases are attempted for the duration of GPS scintillations too. Broadly, it can be observed that 0–1 to 2–3 h durations (lesser) comes in the more poleward magnitudes. Though the argument is not very clear in the case of higher duration events ranging from 3–4 to 5–6 h duration scintillations. However, it can be seen that higher duration events are range from equatorward to poleward wind magnitudes. Thus the nonlinear development of plasma bubbles will be controlled by large poleward winds as well as it can transport the low latitude plasma to regions where recombination is dominant. Subsequently, it can result in the reduction of plasma densities. Hence correspondingly reduced strength and duration of scintillations can be noticed.

Another noteworthy observation of the present study can be considered in the case of wind patterns obtained for mean scintillation vs non scintillation days. The scintillation days are well separated from non scintillation days in terms of magnitude/direction of winds between 18:00 and 20:00LT. Scintillation days are observed to have a clear reduction in the poleward magnitudes around the aforementioned time, whereas the mean winds for non scintillation days are seen to have a clear poleward turning/increment in the poleward wind magnitude. This has significance in the view of presence/absence of GPS scintillations. During a study based on data collected at two American stations between 1996 and 1998 during the equinoxes, Valladares et al. (2002) reported that the averaged meridional wind measured either south or north of Arequipa during mid evening hours on scintillation days are more equatorward than those observed on the nights during no scintillations. Our results are agreeing well with this particular finding, i.e., scintillations days are marked by an reduction in poleward wind in the early night hours while non scintillation days shows an evident increase in the poleward magnitudes. It seems to be unique observation from the Indian sector. During a study of numerical simulations including transequatorial neutral wind effects, Maruyama et al. (2009) suggested that, when the wind velocity was increased from 10 to 40 m/s, corresponding growth time of the plasma bubble was reduced. Thus the larger values of meridional wind velocity and lesser probability of equatorial irregularities obtained in present work is consistent with their study. A study by Muella et al. (2010) over Brazilian stations mentioned that larger poleward wind magnitudes can suppress the EPB development, by controlling the flux tube integrated conductivities, which can reduce the non linear growth of irregularities. The point to note here is that their study considers the stations over two hemispheres as in case of Maruyama et al. (2009). Furthermore, the post midnight equatorward wind magnitudes are also larger for non scintillation days as compared to scintillation days. This point is also in accordance with the observations of Valladares et al. (2002). Thus in this study, we attempt to understand the meridional wind effects on the development of plasma irregularities keeping in mind that the other factors causing day to day variabilities like seed perturbations in the form of gravity waves/other waves in the bottomside F region, variability in zonal winds etc need to be also investigated. While present study focuses on the meridional wind control on ESF during equinoctial months, the understanding of the seasonal behaviour of meridional winds are essential to gain further knowledge of the ESF variations and subsequently to get to know the complete plasma-neutral interactions in the ionospheric region.

5. Conclusions

The present study broadly deals with estimation of meridional winds by considering the h’F values as well as hpF2 values from an equatorial station (TIR) and a low latitude station (HYD) by using motivations from the methods of Murthy et al. (1990) and Rishbeth et al. (1978). Further these derived wind values were compared with HWM07 model. Out of these derived winds, the aim was to understand the effect of wind in affecting the ESF onset/suppression. As a general method, using Superposed Epoch Analysis, the behaviour of winds around the ESF onset were studied. Additionally, the wind variations over the month of May has been obtained which showed a different behaviour. Various characteristics of the meridional winds in terms of h’F and meridional wind velocities have been explored for ESF as well as scintillation events. Meridional wind pattern during March for scintillation and non scintillation events showed remarkable deviations from each other. To conclude, the gross features of the study can be listed as:

(1) Night time meridional winds has been estimated using h’F and hpF2 datas and further compared with HWM07model. While hpF2 derived winds have shifts in their peak, the directions are consistent for both h’F and HWM derived winds, though magnitudes deviates to a certain extent.

(2) In addition, the night time meridional winds during May shows that the wind pattern has changed in such a way that after midnight the wind is not turning to poleward direction, instead they remain equatorward only in most cases.

(3) Superposed Epoch Analysis done for March and April gives the general behaviour of the meridional wind and h’F before and after the ESF onset, which especially for April months shows a clear reduction in poleward wind around 20 min before the ESF onset and thereby rise in h’F which could be attributed to occurence of ESF on most of the days in April.

(4) h’F vs wind values during March and April in terms of ESF duration indicates an interesting feature that for the longer duration events,winds are mainly equatorward or reduced magnitudes of poleward winds. For the shorter duration events, winds are only in the highly poleward values which could have reduced the spread F duration.

(5) The pattern of winds during scintillation days are such that they are spread in range from equatorward to poleward, while it is observed that winds are highly poleward during non scintillation days.

(6) The mean winds derived during March for scintillation days and non scintillation days shows that before ESF onset, winds turned equatorward (reduction in the poleward wind) whereas on non scintillation days and they are characterised by a clear poleward reversal which could reveal the non occurence of scintillations on the particular days.

Acknowledgements

This work is supported by Indian Institute of Geomagnetism under Department of Science and Technology, Government of India. The authors sincerely thank B. Suneel kumar, in-charge, TIFR Balloon facility, Hyderabad for providing ionosonde data from the Hyderabad station. We would like to thank K. Emperumal/C. Selvaraj, Equatorial Geophysical Research Laboratory, Tirunelveli for maintaining CADI ionosonde. The authors would also like to acknowledge the use of MSISE-90 model runs which were obtained from http://omniweb.gsfc.nasa.gov/vitmo/msis_vitmo.html as well as HWM07 model runs.

References

Aarons, J., 1993. The longitudinal morphology of equatorial f-layer irregularities relevant to their occurrence. Space Sci. Rev. 63 (3–4), 209–243.

Abdu, M., Bittencourt, J., Batista, I., 1981. Magnetic declination control of the equatorial f region dynamo electric field development and spread f. J. Geophys. Res.: Space Phys. (1978–2012) 86 (A13), 11443–11446.

Abdu, M., Iyer, K.N., de Medeiros, R., Batista, I.S., Sobral, J.H., 2006. Thermospheric meridional wind control of equatorial spread F and evening prereversal electric field. Geophys. Res. Lett. 33 (7).

Anderson, D., Rusch, D., 1980. Composition of the nighttime ionospheric F 1 region near the magnetic equator. J. Geophys. Res.: Space Phys. (1978–2012) 85 (A2), 569–574.

Banks, P.M., Kockarts, G., 1973. Aeronomy. Academic, New York.

Basu, B., Coppi, B., 1999. Relevance of plasma and neutral wind velocities to the topology and the excitation of modes for the onset of the equatorial spread f. J. Geophys. Res.: Space Phys. (1978–2012) 104 (A1), 225–231.

Batista, I.S., Sastri, J., Medeiros, R.d., Abdu, M., 1997. Nighttime thermospheric meridional winds at cachoeira paulista (23 s, 45 w): evidence for effects of the equatorial midnight pressure bulge. J. Geophys. Res.: Space Phys. (1978–2012) 102 (A9), 20059–20062.

Biondi, M., Meriwether, J., Fejer, B., Woodman, R., 1988. Measurements of the dynamics and coupling of the equatorial thermosphere and the f-region ionosphere in Peru. J. Atmos. Terr. Phys. 50 (10), 937–942.

Bittencourt, J., Abdu, M., 1981. A theoretical comparison between apparent and real vertical ionization drift velocities in the equatorial f region. J. Geophys. Res.: Space Phys. 86 (A4), 2451–2454.

Bittencourt, J., Sahai, Y., 1978. F-region neutral winds from ionosonde measurements of hmf2 at low latitude magnetic conjugate regions. J. Atmos. Terr. Phys. 40 (6), 669–676.

Buonsanto, M., Starks, M., Titheridge, J., Richards, P., Miller, K., 1997. Comparison of techniques for derivation of neutral meridional winds from ionospheric data. J. Geophys. Res.: Space Phys. (1978–2012) 102 (A7), 14477–14484.

Burnside, R., Walker, J., Behnke, R., Gonzales, C., 1983. Polarization electric fields in the nighttime f layer at arecibo. J. Geophys. Res.: Space Phys. (1978–2012) 88 (A8), 6259–6266.

Colerico, M., Mendillo, M., Nottingham, D., Baumgardner, J., Meriwether, J., Mirick, J. Biondi, M., 1996. Coordinated measurements of f region dynamics related to the thermospheric midnight temperature maximum. J. Geophys. Res.: Space Phys. (1978–2012) 101 (A12), 26783–26793.

Devasia, C., Jyoti, N., Subbarao, K., Viswanathan, K., Tiwari, D., Sridharan, R., 2002. On the plausible linkage of thermospheric meridional winds with the equatorial spread f. J. Atmos. Sol. Terr. Phys. 64 (1), 1–12.

Fagundes, P.R., Sahai, Y., Medeiros, R.T., Batista, I.S., Bittencourt, J.A., Takahashi, H., 1997. Nighttime f2-layer peak height changes due to thermospheric winds. Adv. Space Res. 20 (6), 1141–1144.

Fejer, B.G., 1991. Low latitude electrodynamic plasma drifts: a review. J. Atmos. Terr. Phys. 53 (8), 677–693.

Fejer, B.G., Kelley, M., 1980. Ionospheric irregularities. Rev. Geophys. 18 (2), 401–454.

Ganguly, S., Walker, J., Rishbeth, H., 1980. The dynamic f2-layer over arecibo. J. Atmos. Terr. Phys. 42 (6), 553–562.

Gurubaran, S., Sridharan, R., 1993. Effect of meridional winds and neutral temperatures on the f layer heights over low latitudes. J. Geophys. Res.: Space Phys. (1978–2012) 98 (A7), 11629–11635.

Hari, S., Murthy, B.K., 1995. Seasonal variations of equatorial night-time thermospheric meridional winds. J. Atmos. Terr. Phys. 57 (11), 1241–1246.

Harper, R., 1973. Nighttime meridional neutral winds near 350 km at low to mid-latitudes. J. Atmos. Terr. Phys. 35 (11), 2023–2034.

Hedin, A.E., Biondi, M., Burnside, R., Hernandez, G., Johnson, R., Killeen, T. Sica, R., 1991. Revised global model of thermosphere winds using satellite and ground-based observations. J. Geophys. Res.: Space Phys. (1978–2012) 96 (A5), 7657–7688.

Huang, C., Burke, W., Machuzak, J., Gentile, L., Sultan, P., 2002. Equatorial plasma bubbles observed by dmsp satellites during a full solar cycle: toward a global climatology. J. Geophys. Res.: Space Phys. (1978–2012) 107 (A12), SIA–7.

Huba, J., Krall, J., 2013. Impact of meridional winds on equatorial spread f: revisited. Geophys. Res. Lett. 40 (7), 1268–1272.

Hutchinson, J.A., Wright, D., Milan, S., 2011. Geomagnetic storms over the last solar cycle: a superposed epoch analysis. J. Geophys. Res.: Space Phys. (1978–2012) 116 (A9).

Jyoti, N., Devasia, C., Sridharan, R., Tiwari, D., 2004. Threshold height (h? f) c for the meridional wind to play a deterministic role in the bottom side equatorial spread F and its dependence on solar activity. Geophys. Res. Lett. 31 (12).

Krall, J., Huba, J., Joyce, G., Zalesak, S., 2009. Three-dimensional simulation of equatorial spread-f with meridional wind effects. Ann. Geophys 27 (5), 1821–1830.

Krishna Murthy, B., Hari, S., Somayajulu, V., 1990. Nighttime equatorial thermospheric meridional winds from ionospheric h'f data. J. Geophys. Res.: Space Phys. (1978–2012) 95 (A4), 4307–4310.

Liu, L., Luan, X., Wan, W., Lei, J., Ning, B., 2003. Seasonal behavior of equivalent winds over wuhan derived from ionospheric data in 2000–2001. Adv. Space Res. 32 (9), 1765–1770.

Maruyama, T., 1988. A diagnostic model for equatorial spread f, 1, model description and application to electric field and neutral wind effects. J. Geophys. Res.: Space Phys. (1978–2012) 93 (A12), 14611–14622.

Maruyama, T., Saito, S., Kawamura, M., Nozaki, K., Krall, J., Huba, J., 2009. Equinoctial asymmetry of a low-latitude ionosphere–thermosphere system and equatorial irregularities: evidence for meridional wind control. Annales Geophysicae, vol. 27. Copernicus GmbH, pp. 2027–2034.

Medeiros, R.d., Abdu, M., Batista, I., 1997. Thermospheric meridional wind at low latitude from measurements of f layer peak height. J. Geophys. Res.: Space Phys. (1978–2012) 102 (A7), 14531–14540.

Mendillo, M., Baumgardner, J., Pi, X., Sultan, P.J., Tsunoda, R., 1992. Onset conditions for equatorial spread f. J. Geophys. Res.: Space Phys. (1978–2012) 97 (A9), 13865–13876.

Meriwether, J., Heppner, J., Stolarik, J., Wescott, E., 1973. Neutral winds above 200 km at high latitudes. J. Geophys. Res. 78 (28), 6643–6661.

Miller, K., Torr, D., Richards, P., 1986. Meridional winds in the thermosphere derived from measurement of f 2 layer height. J. Geophys. Res.: Space Phys. (1978–2012) 91 (A4), 4531–4535.

Muella, M., Fagundes, P., Bittencourt, J., Sahai, Y., Lima, W., Becker-Guedes, F., Pillat, V., 2008. Nighttime thermospheric meridional neutral winds inferred from ionospheric h? f and hpf2 data. Adv. Space Res. 41 (4), 599–610.

Muella, M.T.d.A.H., de Paula, E., Fagundes, P., Bittencourt, J., Sahai, Y., 2010. Thermospheric meridional wind control on equatorial scintillations and the role of the evening f-region height rise, e× b drift velocities and f2-peak density gradients. Surv. Geophys. 31 (5), 509–530.

Rastogi, R., 1980. Seasonal and solar cycle variations of equatorial spread-f in the american zone. J. Atmos. Terr. Phys. 42 (7), 593–597.

Rishbeth, H., 1967. The effect of winds on the ionospheric f2-peak. J. Atmos. Terr. Phys. 29 (3), 225–238.

Rishbeth, H., Edwards, R., 1989. The isobaric f2-layer. J. Atmos. Terr. Phys. 51 (4), 321–338.

Rishbeth, H., Ganguly, S., Walker, J., 1978. Field-aligned and field-perpendicular velocities in the ionospheric f2-layer. J. Atmos. Terr. Phys. 40 (7), 767–784.

Sahai, Y., Takahashi, H., Fagundes, P., Clemesha, B., Teixeira, N., Bittencourt, J., 1992. Observations of thermospheric neutral winds at 23° s. Planet. Space Sci. 40 (6), 767–773.

Salah, J., Holt, J., 1974. Midlatitude thermospheric winds from incoherent scatter radar and theory. Radio Sci. 9 (2), 301–313.

Sastri, J., Sasidharan, K., Subrahmanyan, V., Rao, M.S., 1979. Seasonal and sunspot-cycle effects in the occurrence of equatorial spread-f configurations. Indian J. Radio Space Phys. 8, 135–138.

Sastri, J.H., Ranganath Rao, H., Somayajulu, V., Chandra, H., 1994. Thermospheric meridional neutral winds associated with equatorial midnight temperature maximum (mtm). Geophys. Res. Lett. 21 (9), 825–828.

Sekar, R., Sridharan, R., 1992. Validity of the estimates of night-time meridional winds made from bottomside ionograms. J. Atmos. Terr. Phys. 54 (9), 1197–1199.

Singer, W., Bremer, J., Hoffmann, P., Manson, A., Meek, C., Schminder, R.Muller, H., 1994. Geomagnetic influences upon tides?winds from mlt radars. J. Atmos. Terr. Phys. 56 (10), 1301–1311.

Sipler, D., Biondi, M., Roble, R., 1983. F-region neutral winds and temperatures at equatorial latitudes: measured and predicted behaviour during geomagnetically quiet conditions. Planet. Space Sci. 31 (1), 53–66.

Spencer, N., Carignan, G., Mayr, H., Niemann, H., Theis, R., Wharton, L., 1979. The midnight temperature maximum in the earth's equatorial thermosphere. Geophys. Res. Lett. 6 (6), 444–446.

Sreeja, V., Devasia, C., Ravindran, S., Sridharan, R., 2009. The persistence of equatorial spread f-an analysis on seasonal, solar activity and geomagnetic activity aspects. Annales Geophysicae, vol. 27. Copernicus Group, pp. 503–510.

Sridharan, R., Gurubaran, S., Raghavarao, R., Suhasini, R., 1991. Coordinated thermospheric and f-region measurements from low latitudes. J. Atmos. Terr. Phys. 53 (6), 515–519.

Sultan, P., 1996. Linear theory and modeling of the Rayleigh–Taylor instability leading to the occurrence of equatorial spread f. J. Geophys. Res.: Space Phys. (1978–2012) 101 (A12), 26875–26891.

Titheridge, J., 1995. The calculation of neutral winds from ionospheric data. J. Atmos. Terr. Phys. 57 (9), 1015–1036.

Valladares, C., Meriwether, J., Sheehan, R., Biondi, M., 2002. Correlative study of neutral winds and scintillation drifts measured near the magnetic equator. J. Geophys. Res.: Space Phys. (1978–2012) 107 (A7), SIA–7.

Yokoyama, N., Kamide, Y., 1997. Statistical nature of geomagnetic storms. J. Geophys. Res.: Space Phys. (1978–2012) 102 (A7), 14215–14222.